DEUTSCHES ELEKTRONEN-SYNCHROTRON

DESY 01–063
May 2001

Generation of High Power Femtosecond Pulses by Sideband-Seeded X-Ray FEL

W. Brefeld, B. Faatz, J. Feldhaus, M. Körfer, T. Möller, J. Pflueger, J. Rossbach, E. L. Saldin, E. A. Schneidmiller, S. Schreiber

Deutsches Elektronen-Synchrotron DESY, Hamburg

J. Krzywinski

Institute of Physics, Polish Academy of Sciences, Warsaw, Poland

M. V. Yurkov

Joint Institute for Nuclear Research, Dubna, Moscow, Russia

ISSN 0418-9833

NOTKESTRASSE 85 - 22607 HAMBURG

To be sure that your reports and preprints are promptly included in the HEP literature database
send them to (if possible by air mail):

DESY
Zentralbibliothek
Notkestraße 85
22603 Hamburg
Germany

DESY
Bibliothek
Platanenallee 6
15738 Zeuthen
Germany

DESY 01-063
May 2001

ISSN 0418-9833

Generation of High Power Femtosecond Pulses by Sideband-Seeded X-ray FEL

W. Brefeld [a] B. Faatz [a], J. Feldhaus [a], M. Körfer [a], J. Krzywinski [b], T. Möller [a], J. Pflueger [a], J. Rossbach [a], E.L. Saldin [a], E.A. Schneidmiller [a], S. Schreiber [a], and M.V. Yurkov [c]

[a] *Deutsches Elektronen-Synchrotron (DESY), Hamburg, Germany*

[b] *Institute of Physics of the Polish Academy of Sciences, 02688 Warszawa, Poland*

[c] *Joint Institute for Nuclear Research, Dubna, 141980 Moscow Region, Russia*

Abstract

New proposal of a fs X-ray facility, which is described in this paper, is based on the use of X-ray SASE FEL combined with a fs quantum laser. An ultrashort laser pulse is used for modulation of the energy and density of the electrons within a slice of the electron bunch at a frequency ω_{opt}. The density modulation exiting the modulator (energy-modulation undulator and dispersion section) is about 10%. Following the modulator the beam enters an X-ray SASE FEL undulator, and is bunched at a frequency ω_0. This leads to an amplitude modulation of the beam density at the sidebands $\omega_0 \pm \omega_{opt}$. The sideband density modulation takes place at the part of the electron pulse defined by the duration of the seed laser pulse that is much shorter than the electron pulse. Following the SASE FEL undulator the beam and SASE radiation enter undulator section (radiator) which is resonant at the frequency $\omega_0 - \omega_{opt}$. Because the beam has a large component of bunching at the sideband, coherent emission is copiously produced within fs slice of the electron bunch. Separation of the sideband frequency from the central frequency by a monochromator is used to distinguish the fs pulses from the sub-ps intense SASE pulses. In this paper we analyze a possibility for integration of fs facility into the soft X-ray SASE FEL at the TESLA Test Facility (TTF) at DESY. Based on the parameters of the SASE FEL and laser pulses of 30 fs duration and 6 μJ energy at a repetition rate of 10 kHz (from Ti:sapphire laser system), it should be possible to achieve an average brilliance of 10^{22} photons $s^{-1}mrad^{-2}mm^{-2}$ per 0.1% BW. The fs source, which is described in this paper, will provide soft X-ray pulses with 30 fs (FWHM) duration. The average number of photons at the monochromator exit can exceed 10^{11} photons per pulse. The fs facility at the TTF is designed to be tunable in the photon energy range 25-100 eV. Present conceptual design is compatible with Phase I and Phase II (self-seeding scheme) of X-ray SASE FEL at the TTF.

Preprint submitted to Nucl. Instrum. and Methods A *25 April 2001*

1 Introduction

Phase transitions, surface processes, and chemical reactions are ultimately driven by the motion of atoms on the time scale of one vibration period ($\simeq$ 100 fs). Unfortunately, the pulse length of existing synchrotron sources is too long for resolving atomic motion on the 100 femtosecond time scale. Recent efforts at applying 300 fs X-rays pulses to probe structural dynamics have used a synchrotron source combined with a femtosecond optical quantum laser [1]. Femtosecond synchrotron radiation pulses were generated directly from an electron storage ring (ALS). An ultrashort laser pulse was used to modulate the energy of electrons within a 100-fs slice of the stored 30-ps electron bunch. The energy-modulated electrons were spatially separated from the long bunch and used to generate 300-fs X-ray pulses at the bending magnet beamline. The same technique can be used to generate 100 fs X-ray pulses of higher flux and brightness with undulator. On the basis of the parameters of an ALS small-gap undulator and laser pulses of 25 fs and 100 μJ at a repetition rate of 20 kHz, one can expect in the future an average brilliance of 10^{11} photons $s^{-1}mrad^{-2}mm^{-2}$ per 0.1 % BW at the photon energy of 2 keV [1].

Another proposal of femtosecond synchrotron radiation soft X-ray facility is based on the use of a linac as a driver [2]. Proposed technique includes the generation of energy chirped short electron bunches that would subsequently spontaneously radiate frequency chirped soft X-ray pulses in an undulator. These pulses are then spectrally dispersed using grazing incident grating. The spectrum is propagated through an exit slit (spectral window) which filters the fs pulses. The shortest temporal structures (about 10 fs) are limited by the energy chirp and longitudinal emittance of the electron bunch, number of undulator periods, and resolution of the monochromator. Potential of the Tesla Test Facility (TTF) at DESY for construction of such a femtosecond X-ray facility has been analyzed in [2]. On the basis of the TTF linac parameters it should be possible to achieve an average brilliance of 10^{14} photons $s^{-1}mrad^{-2}mm^{-2}$ per 0.1% BW in the photon energy range 50-200 eV. The average number of photons at the monochromator exit (at the monochromator efficiency 10%) can exceed 10^5 photons within 30 fs pulse. The pulse duration can be tuned by changing the resolution of the monochromator (by means of changing the spectral window) from 30 fs to 160 fs.

Papers [3,4] discuss how to use an X-ray SASE FEL to produce high power femtosecond pulses. The possibility of producing femtosecond pulses by chirping and compressing (in grazing incidence grating compressor) the output X-ray SASE FEL radiation is analyzed in [3]. Proposed technique includes the generation of energy chirped short electron bunches that would subsequently coherently radiate frequency chirped X-ray pulses in an undulator. Another idea for production of femtosecond high power X-ray pulses is based on a technique of "manipulating" the energy spread along the electron bunch

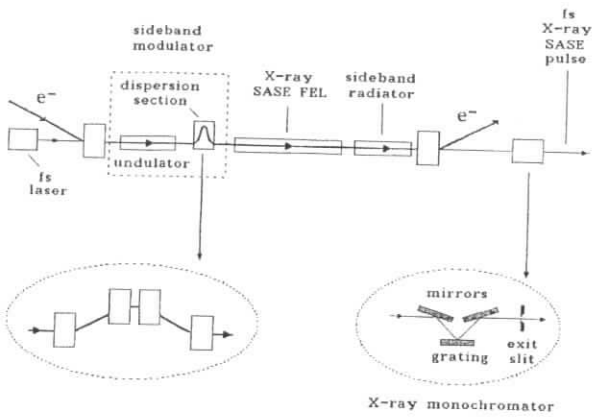

Fig. 1. Basic scheme of a sideband seeded SASE FEL

[4]. Since the radiation amplification process in the SASE FEL is extremely sensitive to the value of the energy spread, only that part of the electron bunch radiates which has low energy spread. Extension of the soft X-ray SASE FEL at the TTF at DESY for generation of high power femtosecond pulses is analyzed in [4]. A novel technique is proposed for preparation of electron bunches with required shaping of the energy spread. On the basis of the TTF parameters it should be possible to achieve an average brilliance of 10^{22} photons $s^{-1}mrad^{-2}mm^{-2}$ per 0.1 % BW. The average number photons can exceed 10^{12} within 30 fs (FWHM) pulse duration.

In this paper we propose sideband seeded X-ray SASE FEL capable to produce femtosecond pulses (see Fig. 1). An ultrashort laser pulse is used to modulate the density of electrons within a femtosecond slice of the electron bunch at a frequency ω_{opt}. We begin the FEL operation by positioning the interaction region on the electron bunch. The seed laser pulse will be timed to overlap with central area of the electron bunch. This ultrashort laser pulse serves as a seed for modulator which consists of an uniform (energy-modulation) undulator and a dispersion section. The interaction of seed pulse with the electron beam produces an energy modulation at ω_{opt}. This energy modulation is converted into a spatial bunching in the dispersion section. Density modulation at the modulator exit is about 10%. The energy modulation, introduced by the modulator, is smaller than the initial energy spread. Following the modulator the beam and seed radiation enter SASE undulator which is resonant with X-ray radiation at frequency ω_0. The process of amplification of the radiation in the X-ray undulator develops in the same way as in the conventional SASE FEL: fluctuations of the electron beam current density serve as the input signal. The seeding optical radiation does not interact with the electron beam in

the X-ray undulator and is diffracted out of the electron beam. By the time the beam is bunched in the SASE FEL undulator at frequency ω_0, the X-ray radiation power has reached saturation. This leads to amplitude modulation of density at the sidebands ($\omega_0 \pm \omega_{opt}$). The sideband density modulation takes place only at that part of the electron bunch defined by the length of the seed laser pulse that is much shorter than the electron bunch. Following the SASE FEL undulator the beam and X-ray radiation enter undulator section (radiator) which is resonant with the $\omega_0 - \omega_{opt}$ radiation. Because the beam has a relatively large component of bunching at the long wavelength sideband, coherent emission at $\omega_0 - \omega_{opt}$ is copiously produced within femtosecond slice of electron bunch. After leaving the radiator the electron beam is deflected onto a beam dump, while the photon beam enters the monochromator, which selects fs soft X-ray pulse.

In this paper we analyze a possibility for integration of proposed femtosecond facility into the soft X-ray SASE FEL being under construction at the TESLA Test Facility at DESY. On the basis of the parameters of TTF SASE FEL and laser pulses of 30 fs duration and 6 μJ energy at a repetition rate of 10 kHz (from a Ti:sapphire laser system), it should be possible to achieve an average brilliance of 10^{22} photons $s^{-1}mrad^{-2}mm^{-2}$ per 0.1 % BW in the photon energy range 25-100 eV. The femtosecond SASE FEL will provide soft X-ray pulses with 30 fs (FWHM) duration. The number of photons at the monochromator exit (at monochromator efficiency 10%) can exceed 10^{11} per pulse which is by three orders of magnitude above the background. This creates perfect conditions for experiments. It is important to notice that the proposed femtosecond option of SASE FEL at the TTF is an additional to a fully functioning SASE FEL improving the output radiation beam properties considerably and thus extending the range of possible applications.

The paper is organized as follows. In Sec. 2 we describe the basic ideas of the proposal. In section 3 we consider the issue of modeling the basic FEL interactions. An introductory section 3.1 provides an overview of FEL physics, concentrating on modeling issues pertinent to the performance of femtosecond FEL. Next, in sections 3.2 and 3.3 we describe the modification of the simulation code in order to include sideband generation from optical laser seed. The femtosecond FEL parameter optimization and performance characterization are described in section 3.4.

2 General description of femtosecond X-ray FEL option at TTF

The main goal of the present study has been to design a femtosecond soft X-ray facility which is compatible with the layout of the TTF and the soft X-ray FEL being under construction at DESY, and which can be realized with minimal additional efforts. The first goal of the TTF FEL is to reach SASE

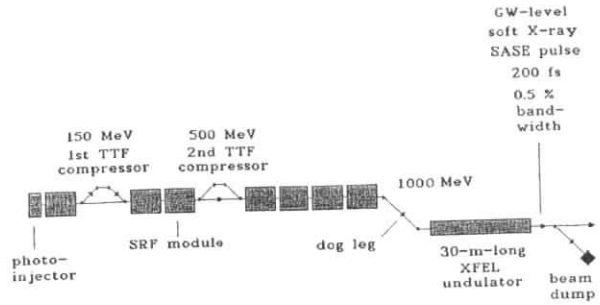

Fig. 2. Schematic layout of the soft X-ray SASE FEL facility (Phase I)

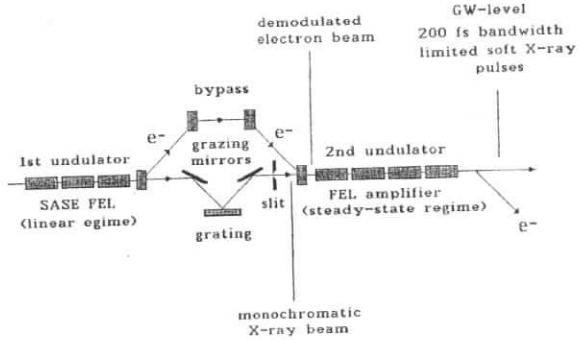

Fig. 3. Schematic layout of the soft X-ray SASE FEL facility with self-seeding option (Phase II)

FEL saturation in the soft X-ray range with six undulator modules (Phase I [5]), and in the second phase to built fully coherent soft X-ray facility based on an idea of the self-seeding option (Phase II [6,7]). The X-ray self-seeding scheme consists of two undulators (four and five modules, respectively), and electron bypass and X-ray monochromator located between them. The layout of the soft X-ray SASE FEL facility at TTF without and with self-seeding option is shown in Figs. 2 and 3, respectively.

Figures 4 and 5 illustrate how the proposed femtosecond facility fits the TTF FEL layout for Phase I and Phase II. This design makes use of the spent electron beam leaving the SASE FEL. An additional facility to be installed is a sideband modulator and sideband radiator. The sideband modulator is located in front of main undulator and consists of 0.4 m long undulator (magnetic period length $\lambda_w = 7.5$ cm, the maximum value of magnetic field is $H_w = 0.7$ T) and 0.5 m long dispersion section (chicane consisting of permanent magnets). The sideband radiator is located after the main undulator and consists of one

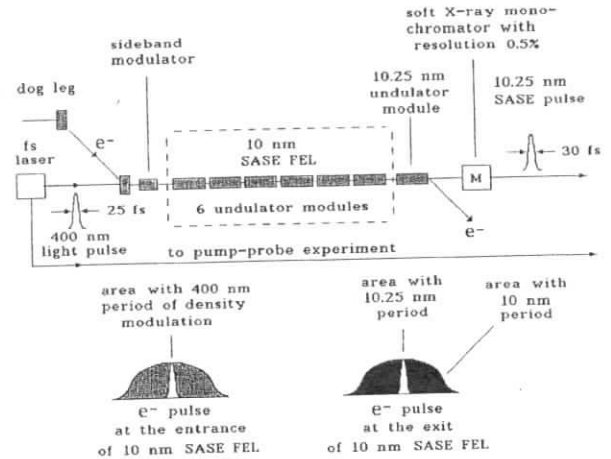

Fig. 4. Schematic layout of the femtosecond pump-probe facility which fits with soft X-ray SASE FEL (Phase I)

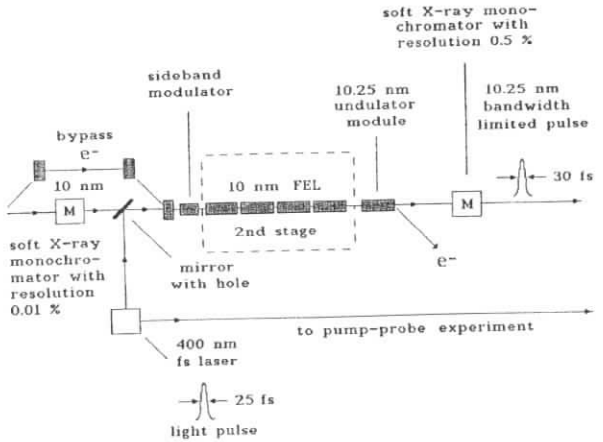

Fig. 5. Schematic layout of the femtosecond pump-probe facility which fits with self-seeding option of soft X-ray SASE FEL (Phase II)

or two 4.5 m standard TTF undulator modules ($\lambda_w = 2.73$ cm, $H_w = 0.51$ T) tuned to the sideband frequency. In this conceptual design we assume to use a Ti:sapphire laser system as a seed laser, which provides at 400 nm wavelength (the 800 nm pulses will be doubled to 400 nm in a frequency conversion crystal) a train of 30 fs pulses with 6 μJ optical energy per pulse, at 10 kHz repetition rate. The installation of the femtosecond seeding system is greatly facilitated

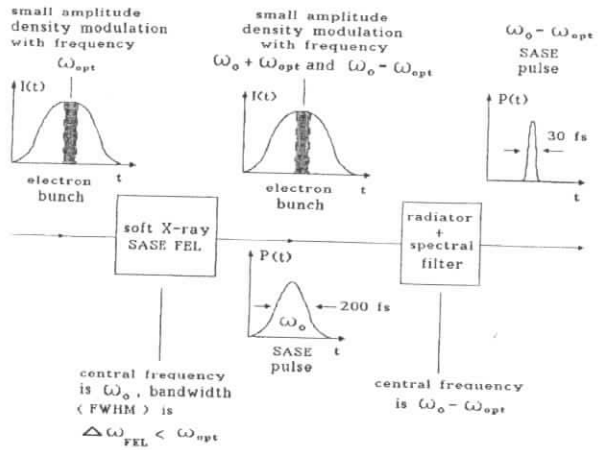

Fig. 6. Sketch of femtosecond soft X-ray pulse synthesation through sideband generation and spectral filtering

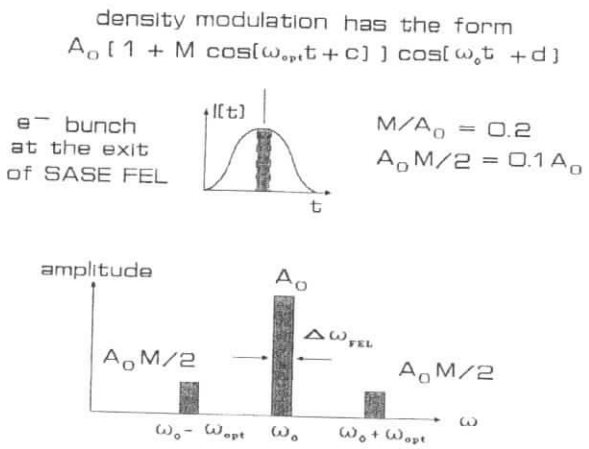

Fig. 7. Summary of the description of the sideband generation for the case of the density modulation as initial conditions.

by the fact that present design of the SASE FEL at TTF provides required free space for the input optical elements and sideband modulator.

Femtosecond soft X-ray pulse synthesation through sideband generation and spectral filtering in sketched in Figs. 6 and 7. The sideband seeded SASE FEL operates as follows (to be specific, we consider the case of 10 nm SASE

FEL). The seed laser pulse is timed to overlap with central area of electron bunch. This ultrashort laser pulse interacts with the electron beam in the short modulator undulator, which is tuned to be resonant to 400 nm. The resulting energy modulation (about 0.5 MeV) is then converted to spatial bunching while the electron beam traverses a dispersion section (a three-dipole chicane). Density modulation at the chicane exit is about 20%. Following the modulator the beam and seed radiation enter SASE undulator which is resonant with X-ray radiation at 10 nm. The process of amplification of the radiation in the 10 nm undulator develops in the same way as in the conventional SASE FEL: fluctuations of the electron beam current density serve as the input signal. The 400 nm seeding optical radiation does not interact with the electron beam in the 10 nm undulator and is diffracted out of the electron beam. By the time the beam is bunched in the SASE FEL undulator at 10 nm, the X-ray radiation power has reached GW level. This leads to amplitude modulation of density at the sidebands 10 ± 0.25 nm. The sideband density modulation takes place at the 30 fs part of the electron pulse, defined by the duration of the seed laser pulse that is much shorter than electron pulse (400 fs FWHM). When this coherently bunched beam enters the sideband radiator undulator there is a rapid coherent generation of 10.25 nm radiation. For an optical wavelength 400 nm, the peak-to-sideband separation has a value of 2.5% . Monochromator with resolution 0.5% located at the end of beamline provides a means for selecting radiation originating from different frequency regions of radiation spectrum. Because the SASE FEL bandwidth (about 0.5 % FWHM) is much less than the separation of the sidebands from the main peak, we obtain clean fs pulse after the monochromator.

The wavelength of femtosecond soft X-ray pulses can be tuned continuously in a wide range. At fixed gaps of the modulator undulator and the sideband radiator undulator the tunability of the output radiation is provided by changing simultaneously the electron energy and the wavelength of the seed laser. In this case the sideband radiator undulator is a version of the standard TTF FEL undulator module with the peak magnetic field on axis a few per cent larger comparing with the main undulator. This undulator can be realized with minimal additional efforts. It should be noticed that the problem of a powerful tunable fs seed laser is not a simple one. In particular, this requires the development and construction of a high peak power optical parametric amplifier (OPA). Fortunately, required parameters for OPA are close to those of OPA developed for the pump-probe facility at the TESLA Test Facility [8]. An additional possibility of variable gap modulator undulator and radiator undulator would allow to increase further the tunability of output radiation from the sideband seeded SASE FEL. Application of both methods (variable gap modulator and radiator undulator and tunable seed laser) would allow to cover the wavelength range of the sideband seeded SASE FEL at TTF from 40 to down 10 nm.

The synchronization of the optical laser with the electron pulses to within

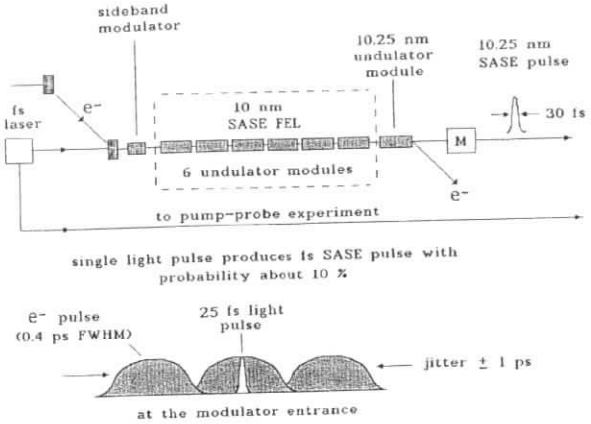

Fig. 8. Effect of a electron pulse jitter on the femtosecond soft X-ray facility if a single optical pulse is used as a seed signal

200 fs is the most challenging task of this proposal. Femtosecond pulses from the laser system should be synchronized to the photoinjector master clock with phase-locking technique. The main problem is the time jitter (± 1 ps) of electron and seed laser pulses. The jitter of electron pulses originates in the photoinjector laser system (laser pulse jitter) and in the magnetic bunch compressors (from predicted $\pm 0.1\%$ electron bunch energy jitter). Due to this uncertainty not every femtosecond optical pulse will produce femtosecond X-ray pulse. The predicted probability of positioning the interaction region on the electron bunch is about 10% only, as can be verified easily from the sketch in Fig. 8. Random production of femtosecond soft X-ray pulses needs to be controlled. A basic question at this point is how femtosecond soft X-ray pulses will be identified. Separation of the sideband frequency from the central frequency can be used to distinguish the 30-fs pulses from the intense 200-fs SASE pulses. I.e., appearing of X-ray pulse at the sideband frequency will indicate that the seed optical pulse is overlapped with the central part of the electron bunch. Moreover, this also indicates that the seed optical pulse and output fs X-ray pulse are synchronized with an accuracy better than 30 fs.

Pump probe techniques which are commonly used with optical lasers, are highly desirable in order to make full use of the femtosecond soft X-ray pulses. Since in this case precise timing is needed with a jitter of less than 30 fs, we suggest to combine the femtosecond soft X-ray pulses with optical pulses generated in the seed laser system. It should be emphasized that in proposed scheme femtosecond X-ray pulse is naturally synchronized with his femtosecond optical pulse and cancel jitter.

In addition, for any experiment in which synchronization with optical fem-

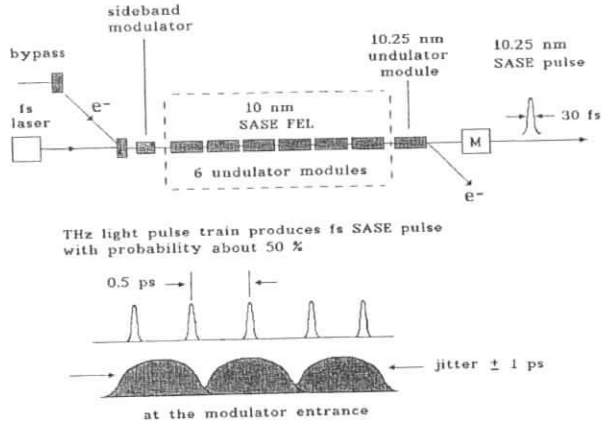

Fig. 9. Effect of a electron pulse jitter on the femtosecond soft X-ray facility if a THz optical pulse train is used as a seed signal

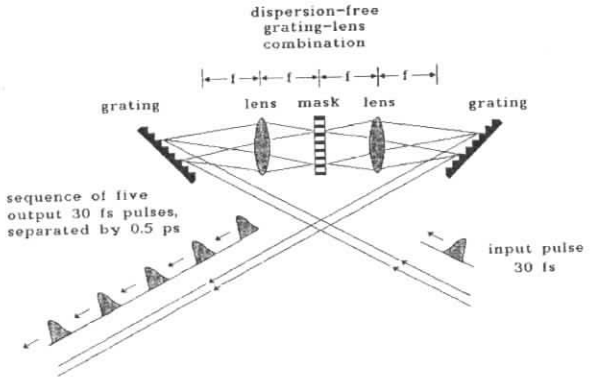

Fig. 10. Typical experimental set-up for THz pulse train generation

tosecond pulse is not critical, THz train of femtosecond optical pulses can be used as a seed signal. For example, if an experiment is not based on the use of pump-probe technique, we can use as a seed signal the sequence of five 30-fs optical pulses, separated by 0.5 ps as illustrated in Fig. 9. In this case probability of positioning interaction region on the electron bunch can be increased up to 50%. A technique best suited for the THz pulse train generation from single fs optical pulse consists of "manipulating" the pulse spectrum in amplitude and phase [9]. The corresponding experimental arrangement is shown in Fig. 10.

Tables 1–3 list some of the basic parameters of the electron beam, un-

Table 1
Parameters of the electron beam at the TESLA Test Facility accelerator

Electron beam

beam energy, MeV	500-1000
bunch charge, nC	1
rms bunch length, μm	50
rms energy spread, MeV	1
normalized emittance, π mm-mrad	2
number of bunches per train	7200
bunch spacing, ns	111
repetition rate, Hz	10

dulators, seed laser system, monochromator and output radiation. Based on the parameters of TTF SASE FEL and laser pulses of 30 fs and 6 μJ at repetition rate of 10 kHz (from a commercially available Ti:sapphire laser system), it should be possible to achieve an average brilliance of 10^{22} photons $s^{-1}mrad^{-2}mm^{-2}$ per 0.1 % BW . For fs facility at TTF, a monochromator and beamline optics, with an overall efficiency of 10 % (30 % grating efficiency and five glancing incidence mirrors at 0.8 reflectivity each) can be used to obtain resolution $\Delta\omega/\omega = 0.5$ % . The femtosecond SASE FEL will provide soft X-ray pulses with 30 fs (FWHM) duration. The average number photons at the monochromator exit can exceed 10^{11} photon/pulse. The femtosecond facility at TTF is designed to be tunable in the photon energy range 25-100 eV.

The design of fs X-ray source, which is described above, makes use of the spent electron beam leaving the X-ray SASE FEL undulator. A more radical solution has been planned to use SASE FEL which operates at 10 nm in the linear regime. In order to obtain saturation at sideband wavelength, the sideband radiator undulator which resonant at 10.25 nm, can be extended by two additional modules. These modification include simultaneously decreasing the number of SASE FEL undulator modules. As a result, there is a space for the possible implementation of a full version to produce high power fs soft X-ray pulses. Fig. 11 presents layout of the full scale fs facility which fits with the self-seeding option (Phase II). In this case we can produce GW level power fs pulses having transform-limited bandwidth.

Here it is relevant to compare scientific capabilities and technical challenges of fs soft X-ray FEL which based on a technique of "manipulating" the energy spread along the electron bunch [4] and sideband seeded fs X-ray FEL which described in this paper. Specific realization of the proposed in [4] fs FEL is compatible with Phase I of X-ray SASE FEL at TTF and can provide soft X-ray pulses with 30 fs (FWHM) duration. Nevertheless, for many applications, one needs to generate a femtosecond scale X-ray pulses. The main advantage of

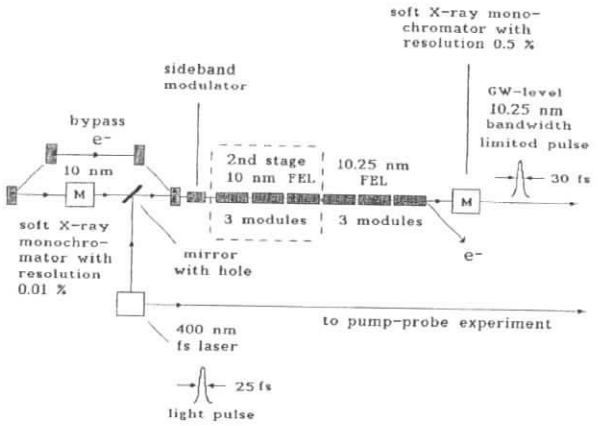

Fig. 11. Possible scenario for the soft X-ray fs pulse power upgrade. Schematic layout of the full scale soft X-ray femtosecond facility which fits with self-seeding option

the scheme, which based on a technique of "manipulating" the energy spread along the electron bunch, is the absence of physical limitations which would prevent operation at very short pulse duration close to the coherence time (of about few fs in our case). The obvious disadvantage of previous conceptual design is the absence of the possibility to integrate this option with Phase II of X-ray SASE FEL at TTF (see Fig. 3). The situation is quite different in the case of femtosecond FEL scheme, which is described in this paper. This design is compatible with Phase I and Phase II of X-ray SASE FEL at TTF. Source, which would involve bandwidth limited 30-fs pulses and shot-to-shot stability, would offer a further major advance in scientific capabilities of X-ray FEL at TTF. Nevertheless, analysis of the practical limit for the achievable pulse duration has shown that there are physical limitations which prohibit attaining femtosecond scale pulse duration. Since the ultrashort optical pulse is used to modulate the density within a slice of electron bunch, the output X-ray pulse duration is limited by the optical pulse duration. A first question that arises is: what is the shortest laser pulse duration? It does not come as surprise that laser pulse duration corresponds to, at least, few optical cycles. In wavelength range 400-800 nm each cycle corresponds to about 1-2 fs. As a result, there is a limitation: At 400 nm wavelength 4 fs pulse duration corresponds to only three optical cycles. A practical limit for achievable pulse duration of Ti:sapphire laser system is about 10 fs. Undulator, which is used for density modulation, must have, at least, few magnetic periods, too. When the electron bunch moves along the undulator, electromagnetic wave advances the electrons by one wavelength at one undulator period. As a result, starting with optical pulse of about 10 fs duration we can obtain minimum about 15 fs pulse duration of the output radiation.

3 FEL Physics and Simulations

In this section we discuss the analysis of the physical processes in the different sections of the sideband seeded SASE FEL, the numerical simulations, and the parameter optimization.

3.1 The physics of femtosecond FEL

This introductory section provides a brief overview of FEL physics, concentrating especially on modeling issue pertinent to the performance of a femtosecond FEL. Let us consider the sideband seeded FEL process. The ultrashort seed laser pulse interacts with the electron beam in the modulator undulator resonant to ω_{opt} and produces an energy and density modulation. The modulated electron beam then passes through the main SASE undulator resonant to ω_0. Upon passing through the main undulator SASE radiation at ω_0 exponentially amplified. This undulator is long enough to reach strong spatial bunching. Finally, a sideband radiator undulator resonant to one of the sidebands $\omega_0 \pm \omega_{opt}$ is used to produce ultrashort radiation pulse.

From the very beginning of this section we combine all the conditions sufficient for the effective operation of a fs SASE FEL. During the passage through a long main SASE undulator the electron density modulation at optical wavelength can be suppressed by energy spread in the electron beam. When the energy spread in the electron beam is Gaussian the suppression factor is given by

$$S = \exp[-\langle(\Delta\mathcal{E})^2\rangle L_{(2)}^2\omega_{opt}^2/(2c^2\gamma_l^4\mathcal{E}_0^2)] ,$$

where $\gamma_l = \gamma/(1+K_{(2)}^2/2)^{1/2}$ is the longitudinal relativistic factor, $K_{(2)}$ and $L_{(2)}$ is the undulator parameter and undulator length, respectively, the subscript (2) refers to the main undulator. For effective operation of the fs FEL energy spread suppression factor should be close to unity. This leads to following condition:

$$\langle(\Delta\mathcal{E})^2\rangle L_{(2)}^2\omega_{opt}^2/(2c^2\gamma_l^4\mathcal{E}_0^2) \ll 1 . \qquad (1)$$

The chosen parameters for the SASE FEL and the seed laser system satisfy this condition, and to make preservation of the beam density modulation in the case of the TTF SASE FEL parameters is possible. Parameters in our case are :

$$\sqrt{\langle(\Delta\mathcal{E})^2\rangle}L_{(2)}/(\gamma_l^2\mathcal{E}_0) \simeq 15 \text{ nm} , \quad \lambda = 2\pi c/\omega_{opt} = 400 \text{ nm} .$$

As a result, $Sa_{opt} \simeq a_{opt}$ and the microbunching is not destroyed when the electron bunch passes the main undulator.

In what follows we use the following assumptions:

$$\omega_0 \gg \omega_{opt} \gg \Delta\omega_{SASE} . \qquad (2)$$

We also assume that

$$\Delta\omega_{SASE} \gg 1/\tau_{opt} \gg 1/\tau_e . \qquad (3)$$

Here τ_{opt} and τ_e is the seed optical pulse and electron pulse duration, respectively. Such assumptions do not reduce significantly the practical applicability of the result obtained. Let us consider condition (2). It is obvious that the parameter ω_{opt}/ω_0 is much less than unity for X-ray SASE FEL. We also assume that the SASE bandwidth is much less than the separation of the sidebands from the main peak. This requirement is of a critical importance to the overall performance of the fs SASE FEL. In this case, monochromator can be used to distinguish the fs pulses from the intense SASE pulses.

Let us discuss the problem of choosing the output radiation wavelength range for the fs SASE FEL. Increase of the operating frequency ω_0 leads to the increase of the SASE bandwidth $\Delta\omega_{SASE}$. In our case, the maximum frequency is limited by the requirement that ratio $\Delta\omega_{SASE}/\omega_{opt}$ must be small. Analysis of parameters of fs X-ray SASE FELs shows that its output radiation wavelength range is limited by the value of about few nm. In order to go to wavelength range beyond nm, the bandwidth of output radiation would therefore be decreased. The development of self-seeding SASE FEL now offers the possibilities of powerful X-ray sources with narrow band of photons. For the self-seeding case, a sub-nm fs FEL based on sideband generation is feasible because of small bandwidth of output radiation $\Delta\omega_{out} \ll \omega_{opt} \ll \Delta\omega_{SASE}$. Fortunately, in the case of the TTF FEL the value of the $\Delta\omega_{SASE}$ is much less than ω_{opt} and our design allows for the future incorporation of fs X-ray SASE FEL option without and with self-seeding scheme.

The present study assumes wavelength of seed light to be very long compared to the SASE radiation wavelength. Under this limitation we neglect the gradient of density and energy within the SASE radiation wavelength at the entrance of main undulator. Due to this reason it is also convenient to describe effect of the energy and density modulation not by energy-phase distribution function, but by periodical bunch profile and periodically correlated energy spread. The physical interpretation of approximation $\Delta\omega_{SASE}/\omega_{opt} \ll 1$ is that the slippage of the radiation with respect to the electrons per gain length (in the SASE FEL) is much longer than the seed laser wavelength.

Let us consider condition (3). It is obvious that the fs FEL has advantage over conventional SASE FEL only when electron bunch is much longer than the seed laser pulse. This allows us to neglect electron bunch profile effects and to use the model of a rectangular electron bunch of sufficient duration T, such as $T > \tau_{opt}$. The physical interpretation of condition $\Delta\omega_{SASE} \gg 1/\tau_{opt}$ is

that the optical pulse is much longer than the slippage of the radiation with respect to the electrons at one gain length.

To obtain clear physical picture, we start with simple physical considerations in the framework of the one dimensional model. In the proceeding sections we confirm them with the results of simulations with three-dimensional, time-dependent simulation code FAST. The main emphasis is put on the description of the sideband effects. One-dimensional model assumes the input shot noise and the output radiation to have full transverse coherence. Let us discuss the region of validity of one-dimensional approximation. The results of one-dimensional calculations can be applied to the fs FEL because the transverse coherence of the radiation is settled at the SASE undulator exit. Thus, the sideband harmonic is also transversely coherent. In frame work of one-dimensional approximation the spectrum of SASE radiation is concentrated within the narrow band, $\Delta\omega_{\rm SASE}/\omega_0 \simeq 0.5\%$, near the resonance frequency. On the other hand, there is a large Fourier harmonic of current at the sideband frequency, and it is well known that the frequency of undulator radiation have a wide spectral width. Taking the frequency as ω_0 on axis ($\theta = 0$), and $\omega_0 - \Delta\omega$ off axis at angle θ, then taking ratios, one obtains

$$\frac{\Delta\omega}{\omega_0} \simeq \gamma_l^2\theta^2 \ , \qquad (4)$$

where this expression shows how the frequency decreases as one observes the radiation off axis. Note that the cone of half-intensity half angle encloses a relative spectral bandwidth of about 25 % [10]. In our case, separation of long wavelength sideband from main peak is $\omega_{\rm opt}/\omega_0 \simeq 2.5\%$ only. So, the reasonable question arises of whether one-dimensional model describes correctly physical process in fs FEL. Simple physical considerations show that this model is valid. The result (4) is for a single electron. A more useful result would be the power radiated by spatially modulated electron bunch. In this case the radiated fields due to different electrons are correlated: that is, we sum fields, not intensities. A large number of transverse radiation modes are excited when the electron beam enters the SASE undulator. These radiation modes have different grows rates. Starting from some undulator length the contribution to the total power of the fundamental ($\rm TEM_{00}$) mode (corresponding to the resonance frequency ω_0) becomes to be dominant. Thus, the sideband harmonic of current density is also transversely coherent and should be distributed according to $\rm TEM_{00}$ eigenfunction. Typical angular divergence of radiation due to diffraction effects is about of $\Delta\theta \simeq \lambda/D$, where D is the transverse size of the radiation beam. In the case of TTF SASE FEL, the diffraction expansion of the radiation at one gain length will be small and transverse size of $\rm TEM_{00}$ mode is close to the transverse size of electron beam ($D \simeq \sigma_e$). As a result, coherent sideband radiation in the SASE undulator should be directed at zero angle within the cone of half angle $\theta \simeq c/(\sigma_e\omega_0)$. On the other hand, this diffraction angle is much smaller comparing with reso-

nance angle, $\theta_{\rm res} \simeq \sqrt{\gamma_l^2\omega_{\rm opt}/\omega_0}$, from (4). Thus, we find that one-dimensional approximation is valid.

Let us begin with a qualitative analysis of sideband generation process. All the formulae refer the case of a planar undulator. The transverse current density may be written in the form

$$j_y = v_y(z)j_z(z,t)/c \ .$$

The velocity components of the electron moving in the field of the planar undulator are given by the expressions:

$$v_x = 0 \ , \quad v_y = -e\theta_l \sin(k_{\rm w}z) \ , \quad v_z = v - \frac{c\theta_l^2}{2}\sin^2(k_{\rm w}z) \ .$$

Here v is the total velocity of the electron. One can obtain that the radiation of the electron beam in the undulator is in resonance with the electron motion when

$$k_{\rm w} + \frac{\omega_0}{c} - \frac{\omega_0}{\bar{v}_z} = 0 \ ,$$

where $\bar{v}_z = v - c\theta_l^2/4$ is the velocity of the electron along the z axis, averaged over undulator period.

The spectrum of the SASE radiation is concentrated within the narrow band near the resonance frequency ω_0. Therefore, the electric field of the wave can be presented as

$$E_y(z,t) = \tilde{E}(z,t)\exp\left[\mathrm{i}\,\omega_0(z/c - t)\right] + \text{C.C.} \ , \qquad (5)$$

where $\tilde{E}$ is the slowly varying complex amplitude:

$$|\partial\tilde{E}/\partial t| \ll \omega_0|\tilde{E}| \ , \quad |\partial\tilde{E}/\partial z| \ll k_{\rm w}|\tilde{E}| \ .$$

It is convenient to write down an expression for the current density in the following form:

$$j_z(z,t) = -j_0 + \tilde{j}_{\rm a}(z,t)\exp\left(\mathrm{i}\,\psi'\right) + \text{C.C.} \ , \qquad (6)$$

where

$$\psi' = k_{\rm w}z + \omega_0(z/c - t) - Q\sin\left(2k_{\rm w}z\right) \ , \quad Q = \frac{\omega_0\theta_l^2}{8k_{\rm w}c} \ ,$$

and $-j_0$ is the current density.

Prior to numerical simulations of the sideband generation process, it is relevant to present a qualitative physical picture. First, we have used the following simplifying assumption about SASE bunching parameter

$$|\hat{a}_0| = |\tilde{j}_{\rm a}(z,t)/j_0| \ll 1 \ .$$

This means that the SASE FEL operates in a linear regime. We use the model of a long electron bunch with rectangular axial profile of current. When the SASE FEL operates without laser modulation, the driving electron beam can be considered as an active medium whose properties do not depend on the time and longitudinal coordinate. In this case investigation of the SASE FEL process is performed with steady-state spectral Green's function connecting the Fourier amplitudes of the output radiation field and the Fourier amplitudes of the input noise signal. Since in the linear regime all the harmonics are amplified independently, we can use the result of steady-state theory for each harmonic and calculate the corresponding Fourier harmonics of output radiation field. Let us analyze the nature of self-consistent solution at exact resonance $\omega = \omega_0$. The bunching parameter at sufficient distance from the (second) undulator entrance can be represented as $\hat{a}_0 = A\exp(\Lambda_0 z)$, where Λ_0 is growing root of eigenvalue equation at exact resonance. Let us now study the influence of seed laser modulation on the spectrum of the beam current. In this case, at the end of the main undulator, there is an energy and density oscillations at the seed laser frequency. In the framework of accepted limitations we consider the case when the bunching parameter $\hat{a}_{\rm opt}$ at the exit of the main undulator is much smaller than unity. The process of sideband generation can be easily understood from analysis of nonlinear current perturbation terms, which are of the order of $\hat{a}_0\hat{a}_{\rm opt}$. If factor $\hat{a}_{\rm opt}$ is much smaller than unity, the effects of density modulation and energy modulation can be studied separately.

Let us consider the current perturbation under the influence of density modulation. In the framework of accepted limitations (2) introducing the density modulation does not change SASE process. Indeed, the present study assumes the slippage of the radiation with respect to the electrons per gain length to be very large compared to optical wavelength. With respect to calculation of SASE FEL process, it allows us to neglect the effect of beam density modulation and to use steady-state Green's function. This qualitative consideration allows one to find sideband harmonic components. Current perturbation at the SASE undulator exit under the influence of seed optical laser is given by

$$j_z(t) = -j_0[1 + 2\mathrm{Re}(\hat{a}_{\rm opt}\exp(\mathrm{i}\,\omega_{\rm opt}t))]\hat{a}_0\exp(\mathrm{i}\,\omega_0 t) + \mathrm{C.C.}$$

The expression in the square bracket is the periodical variation of the bunch profile. Fourier expansion of this function gives the sideband harmonic components of the current converted from the beam profile modulation. Thus, we conclude that the sideband (nonlinear) harmonic current is determined by factor $\hat{a}_0\hat{a}_{\rm opt}$.

Complete calculation of the parameters of the femtosecond X-ray FEL can be performed only with numerical simulation code. In this section we consider one-dimensional model to give an idea about upgrade of a time-dependent code for calculations of the sideband seeded SASE FEL. An extension of this approach to three-dimensional case is straightforward.

Let us start with the solution of the electrodynamic problem. The wave equation for the electromagnetic wave, $\vec{E} = \vec{e}_y E_y(z,t)$, amplified by the electron beam in the planar undulator, has the form:

$$\frac{\partial^2 E_y}{\partial z^2} - \frac{1}{c^2}\frac{\partial^2 E_y}{\partial t^2} = \frac{4\pi}{c^2}\frac{\partial j_y}{\partial t}\,. \tag{7}$$

The solution of wave equation in resonance approximation for the slowly varying amplitudes $\bar{j}_{\rm a}$ and $\tilde{E}$ has the form:

$$\tilde{E}(z,t) = \mathrm{i}\,\frac{\pi\theta_l A_{\rm JJ}}{c}\int\limits_0^z \bar{j}_{\rm a}\left(z', t - \frac{z-z'}{c}\right)\mathrm{d}\,z'\,.$$

where $A_{\rm JJ} = [J_0(Q) - J_1(Q)]$.

The next point is the solution of the dynamical problem. As we have already mentioned, for a particle moving with nominal velocity $\bar{v}_z$ (which corresponds to the nominal energy $\mathcal{E}_0$), the phase ψ' is constant along z. Therefore, $\mathrm{d}\,\psi'/\mathrm{d}\,z \neq 0$ only in the case when the particle energy deviates from the nominal value: $P = \mathcal{E} - \mathcal{E}_0 \neq 0$. Then the equations of motion averaged over an undulator period have the form:

$$\frac{\mathrm{d}\,P}{\mathrm{d}\,z} = -\frac{\mathrm{i}}{2}A_{\rm JJ}e\theta_l\tilde{E}(z,t)\exp(\mathrm{i}\,\psi') + \mathrm{C.C.}\,, \qquad \frac{\mathrm{d}\,\psi'}{\mathrm{d}\,z} = \frac{\omega_0 P}{c\gamma_l^2\mathcal{E}_0}\,.$$

To perform the numerical simulations of fs FEL, we should go over to discrete quantities. Suppose, we have an electron bunch of length $l_{\rm b}$. We divide it into $N_{\rm b} = l_{\rm b}/\lambda$ boxes, where $\lambda = 2\pi c/\omega_0$. When the number of particles in the bunch is equal to N, the number of particles per box is equal to $N_\lambda = N/N_{\rm b}$ (we neglect fluctuations of this number with the relative standard deviation $1/\sqrt{N_\lambda}$, since they are always small). Let us consider the coordinate $s = z - \bar{v}_z t$ and defined the position of the bunch tail as $s = 0$ and that of the bunch head as $s = l_{\rm b}$. Then we assign a number to each box in accordance with the formula $j = [s/\lambda]$, where $[\cdots]$ denotes the integer part of a number. At any fixed point z along the undulator the arrival times of boxes differ by $\Delta t = t_j - t_{j+1} = \lambda/\bar{v}_z$. The position of each particle within the bunch is defined by the box number j and by the phase $0 < \psi' < 2\pi$. Indeed, for a particle moving with nominal energy $\mathcal{E}_0$ (which corresponds to the nominal velocity $\bar{v}_z$) the phase ψ' is constant.

The phase of each particle may be written in the form:

$$\psi' = 2\pi \left\{ \frac{s}{\lambda} - \left[\frac{s}{\lambda} \right] \right\} .$$

Let us now introduce the notion of bunching in jth box:

$$\hat{a}_1^{(j)} = \frac{1}{N_\lambda} \sum_{k=1}^{N_\lambda} \exp\left(-\mathrm{i}\,\psi_k'^{(j)}\right) , \tag{8}$$

where $\psi_k'^{(j)}$ is the phase of the kth particle inside the jth box. The complex amplitudes $\tilde{j}_a$ and $\hat{a}_1$ are connected by the relation:

$$\tilde{j}_a(z, t_j)/j_0 = -\hat{a}_1^j(z) .$$

Let us perform the normalization procedure

$$\hat{z} = \Gamma z , \qquad \hat{P} = P/(\rho \mathcal{E}_0) ,$$

$$\hat{C} = C/\Gamma , \qquad \hat{E} = \tilde{E}/E_0 ,$$

where

$$\Gamma = [\pi j_0 \theta_l^2 \omega_0 A_{JJ}^2 \gamma^{-1} \gamma_l^{-2} I_A^{-1} (2c)^{-1}]^{1/3} ,$$

$$\rho = c\gamma_l^2 \Gamma/c , \qquad E_0 = c\mathcal{E}_0 \gamma_l^2 \Gamma^2/(e\theta_l \omega_0 A_{JJ}) ,$$

$I_A \simeq 17$ kA is the Alphven current. As a result, we can wright the self-consistent equations in the following reduce form:

$$\frac{\mathrm{d}\,\hat{P}_k^{(j)}}{\mathrm{d}\,\hat{z}} = -\frac{\mathrm{i}}{2} \hat{E}^{(j)}(\hat{z}) \exp\left(\mathrm{i}\,\psi_k'^{(j)}\right) + \text{C.C.} , \quad \frac{\mathrm{d}\,\psi_k'^{(j)}}{\mathrm{d}\,\hat{z}} = \hat{P}_k^{(j)} , \tag{9}$$

$$\hat{E}^{(j)}(\hat{z}) = -2\,\mathrm{i}\,\Delta\hat{z} \sum_{m=1}^{n} \hat{a}_1^{(j-m)}(\hat{z} - m\Delta\hat{z}) , \tag{10}$$

where $\hat{E}^{(j)}(\hat{z}) = \tilde{E}(\hat{z}, t_j)/E_0$ is the normalized field in the jth box, $\hat{P}_k^{(j)} = P_k^{(j)}/(\rho\mathcal{E}_0)$ is the normalized energy deviation from the nominal value of the kth particle in the jth box, $\Delta\hat{z} = \Gamma\lambda_w$, and $n = [\hat{z}/\Delta\hat{z}] = [z/\lambda_w]$.

Simultaneous solution of (9) and (10) allows one to calculate the evolution in time and space of the electromagnetic field and of the particle motion under given initial condition at the undulator entrance. The beam bunching is calculated according to (8). The simulation proceeds in the following way. At each integration step over the $\hat{z}$ coordinate the normalized field amplitude is calculated in each box using (10). Then equations (9) for the particle motion are integrated within each box. At the next step of integration, at $\hat{z} + \Delta\hat{z}$, the bunching and the field are recalculated, and the procedure is repeated. In

the code, it is modular from 0 to 2π, and when the particle increases past 2π, the code automatically subtracts 2π to keep it within the range. This time-dependent algorithm was used for simulations of the FEL amplifier starting from shot noise [11].

3.3 Modification of the time-dependent code to include sideband generation

Now we discuss the modifications of described above code required to carry out the calculations of the sideband generation. If electron bunch interacts with laser radiation in the main undulator, one should keep in mind several effects. The first effect is the axial variation of the electron bunch profile. Suppose that the electron bunch at the exit of modulator has a waveform axial profile of the current density:

$$S(s) = -j(s)/j_0 = 1 + \hat{a}_{\mathrm{opt}} \cos(2\pi s/\lambda_{\mathrm{opt}}) ,$$

To simulate the FEL amplifier driven by electron bunch with a gradient profile, we should modify the self-consistent equations. The period of modulation is assumed to be large, $\lambda_{\mathrm{opt}}/\lambda \gg 1$. Under this limitation only equation (10) for the complex field amplitude should be replaced by

$$\hat{E}^{(j)}(\hat{z}) = -2\,\mathrm{i}\,\Delta\hat{z} \sum_{m=1}^{n} S^{(j-m)} \hat{a}_1^{(j-m)}(\hat{z} - m\Delta\hat{z}) , \tag{11}$$

where $S^{(j)}$ is the value of the function $S(s)$ in the jth box.

The second effect is that energy change along the electron bunch, i.e. we need to simulate the microbunching process for the beam with correlated energy spread. Suppose that before entering the radiator undulator, the electron distribution in energy is

$$\hat{P}_c(s) = \frac{\delta\gamma(s)}{\rho\gamma} = \delta\hat{\gamma}_{\mathrm{opt}} \cos(2\pi s/\lambda_{\mathrm{opt}} + \beta) ,$$

where $\delta\hat{\gamma}_{\mathrm{opt}}$ is the energy bunching parameter. We modify the above algorithm to include the correlated energy change effects by introducing the energy shift. When the energy changes along the bunch, the energy shift is a function of the box number j. Following this procedure equation (10) for the phase of the particles inside the jth box should be replaced by

$$\frac{\mathrm{d}\,\psi_k'^{(j)}}{\mathrm{d}\,\hat{z}} = \hat{P}_k^{(j)} + \hat{P}_c^{(j)} , \tag{12}$$

where $\hat{P}_c^{(j)}$ is the value of the function $\hat{P}_c(s)$ in the jth box. Under accepted limitations (3), we neglect the gradient of energy and density on the scale of the box. Therefore, in the code, it is modular from 0 to 2π.

The FEL process in the sideband radiator undulator is calculated in the same way as in the main SASE undulator. The energy-phase distribution of the macroparticles at the exit of the main undulator serves as initial condition for the code. One can note that the algorithm, which was described above, allows one to use any box length (within the narrow band $\Delta\lambda/\lambda \ll 1$). To perform the numerical simulations of the FEL process in the main undulator we use the resonance box length. When preforming numerical simulations of the sideband harmonic generation in the sideband radiator, we continue to use the same box length. As a result, the procedure for preparing initial conditions at the entrance of the sideband radiator undulator becomes pretty simple. For simulation of the resonance frequency shift in the radiator compared to the second undulator we put parameter $\hat{P}_0 = \omega_{opt}/(\rho\omega_0)$ into equation for the phase: $\mathrm{d}\,\psi_k^{\prime(j)}/\mathrm{d}\,\hat{z} = \hat{P}_k^{(j)} + \hat{P}_c^{(j)} + \hat{P}_0$.

3.4 Simulation results

We illustrate operation of a fs option of FEL for parameters of the TTF FEL operating at the wavelength of 20 nm. Parameters of the electron beam are presented in Table 1. Parameters of the optical laser are: wavelength 400 nm, energy in the laser pulse 6 μJ, and FWHM pulse duration 25 fs (see Table 2 and Fig. 12). The laser beam is focused onto the electron beam in a short (five periods) undulator resonant at the optical wavelength of 400 nm. Optimal conditions of focusing correspond to the positioning of the laser beam waist in the center of the undulator. The size of the laser beam waist is twice as large than the electron beam size. Due to the resonant interaction of the electron beam with optical field in the undulator the electron beam is modulated in the energy as it is shown in Fig. 13. Upon leaving the modulator the electron beam passes the dispersion section, is modulated additionally in the density (see Fig. 14), and is directed to an X-ray undulator.

We start with simple one-dimensional model in order to illustrate mechanism of the sideband generation. We assume that there is only main undulator (no sideband radiator undulator installed). We performed three independent simulation runs with different initial conditions:

(a) – the electron beam is modulated in density at the undulator entrance as it is shown in Fig. 14;

(b) – the electron beam is modulated in energy at the undulator entrance as it is shown in Fig. 13;

(c) – the electron beam is modulated in energy and in density at the undulator entrance as it is shown in Figs. 13 and 14;

in order to study which kind of initial conditions is better for the sideband FEL option. Figure 15 shows evolution of the spectral distribution of the beam modulation along the undulator. It is seen that initial conditions (b)

Table 2
Parameters of the sideband modulator

Undulator	
Type	planar
number of periods	5
period, cm	7.5
peak field, T	0.7
external beta-function, m	1.7
Seed laser	
wavelength, nm	400
min. pulse duration, fs (FWHM)	25
energy per pulse, μJ	6
spectrum width	transform limited
rep. rate, kHz	10
time jitter, ps	1

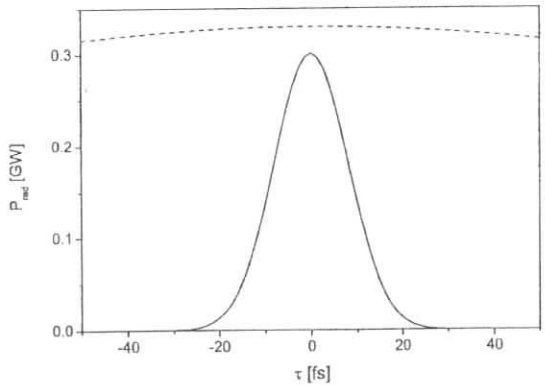

Fig. 12. Laser pulse of the optical seeding laser. Dashed line denotes longitudinal profile of the electron bunch.

give better results with respect to the sideband generation. Simulations show also that joint effect of the initial conditions (a) and (b) (case (c)) results in an additive effect on the sideband generation. We should also stress that initial conditions (a) seed only sidebands at frequencies $\omega_0 \pm \omega_{opt}$, while conditions (b) seed also higher order sidebands. The power of the second order sideband,

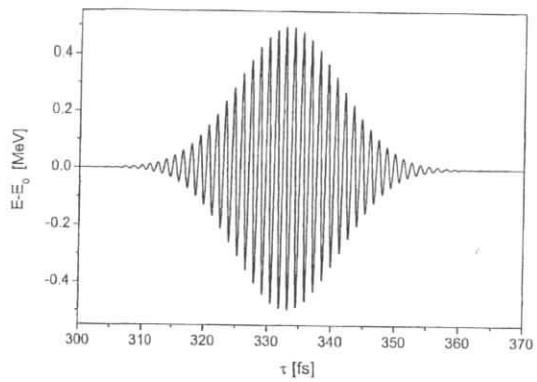

Fig. 13. Energy modulation of the electron beam at the exit of the modulator undulator.

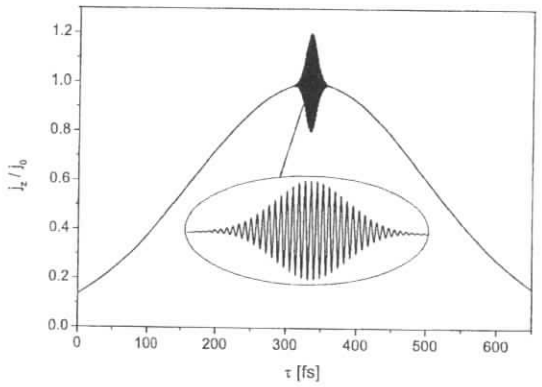

Fig. 14. Density modulation of the electron beam at the exit of the dispersion section.

$\omega_0 \pm 2\omega_{opt}$, is rather high, and it can be used in the sideband-seeded SASE FEL. From practical point of view this means that using the same optical laser we can extend by a factor of two the operating range of fs SASE FEL to shorter wavelengths.

It is seen from Fig. 15 that at the initial stage of amplification spectral purity of the sideband is relatively poor due to the shot noise in the electron beam. In the amplification process it is improved significantly and reaches

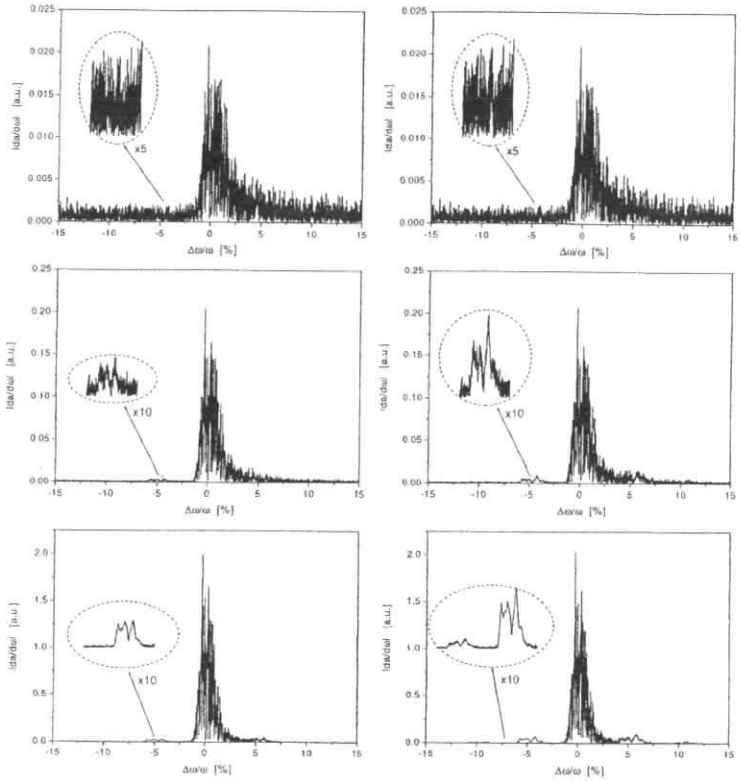

Fig. 15. Spectral distribution of the beam density modulation at different length of main undulator: $\hat{z} = 4.7$, 7.5, and 10.3 (upper, middle and lower plots, respectively). Left column corresponds to initial conditions of the density modulation (see Fig. 14), and right column is the case of the energy modulation (see Fig. 13). Calculations have been performed within framework of one-dimensional model.

maximal value in the end of the linear regime, at $\hat{z} \simeq 10.6$ (saturation takes place at $\hat{z} \simeq 13$). Figure 16 shows additional details of the sideband generation process at this point. Left column in this figure present plots of the microbunching (total and that filtered at the sideband frequency). Plots in the right column refer to the full radiation power and that filtered at the sideband frequency. The spectrally filtered radiation pulse has short pulse duration and good contrast (signal to background ratio) of about 1000.

When the FEL process enters nonlinear stage, an effect of nonlinear sideband generation takes place which leads to decrease of the contrast of the seeded sideband. However, with the help of plots presented in Fig. 17 we can

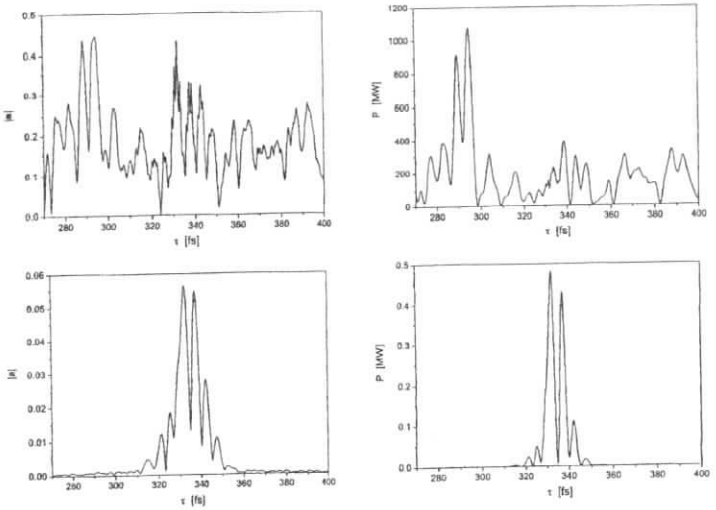

Fig. 16. Details of the sideband generation process at a point corresponding to the maximal contrast of the sideband in the main undulator ($\hat{z} = 10.6$). Left column: plots of the full density modulation and that filtered at the sideband frequency. Right column: full radiation power and that filtered at the sideband frequency. Initial conditions corresponds to general case (c). Calculations have been performed within framework of one-dimensional model.

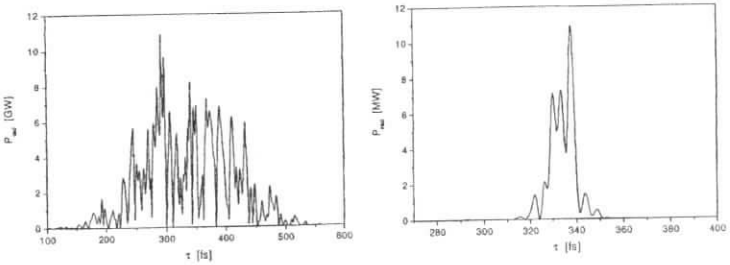

Fig. 17. Left plot: Time structure of the radiation pulse from SASE FEL operating at saturation. Right plot: Radiation pulse after spectral filtering at the sideband frequency. Here the length of the main undulator is equal to $\hat{z} = 13$, and there is no sideband radiator undulator. Initial conditions correspond to general case (c). Calculations have been performed within framework of one-dimensional model.

conclude that at the saturation point the contrast of the radiation pulse produced by the seeded sideband is still high (of about factor of 100), and the peak power of the radiation in the fs pulse can reach the value of a few MW at the exit of the main undulator.

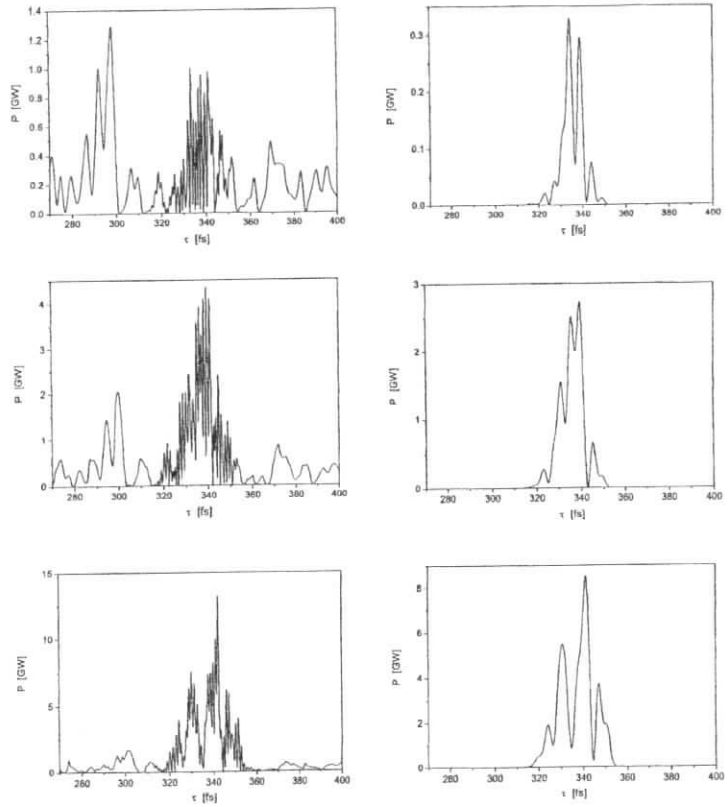

Fig. 18. Evolution of the radiation pulse in the radiator undulator at different length of the radiator undulator: $\hat{z} = 1.5$, 3.3, and 5.2 (upper middle, and lower plots, respectively). In the left plots we present total pulse, and in the right plots – spectrally filtered at the sideband. The length of the main undulator is equal to $\hat{z} = 10.6$ and provides maximum contrast of the sideband. Calculations have been performed within framework of one-dimensional model.

Next problem to be investigated is that to find optimal parameters of the fs FEL consisting of the main undulator and the sideband radiator undulator tuned to the sideband frequency. Simulations show that optimization is rather simple in this case. The length of the main undulator is given by the condition of the maximal purity of the beam density modulation at the sideband which takes place in the end of the linear regime (of about two field gain length before the saturation). Figure 18 show the evolution of the beam modulation

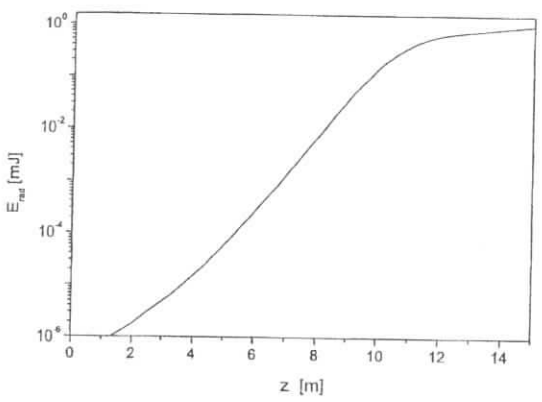

Fig. 19. Energy in the radiation pulse versus undulator length for 20 nm SASE FEL at the TESLA Test Facility. Calculations have been performed with three-dimensional, time-dependent simulation code FAST.

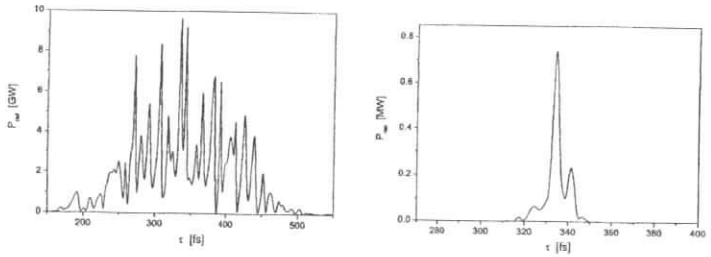

Fig. 20. Left plot: Time structure of the radiation pulse for 20 nm SASE FEL at the TESLA Test FAcility operating at saturation. Right plot: Radiation pulse after spectral filtering at the sideband frequency. Calculations have been performed with three-dimensional, time-dependent simulation code FAST.

density and the radiation power in the sideband radiator undulator. It is seen that proposed techniques allows one to produce fs pulses with output power comparable with the saturation power of the conventional SASE FEL.

Up to now we performed simple physical considerations in the framework of the one-dimensional model in order to prove the principle of sideband generation. Final optimization have been preformed with three-dimensional, time-dependent code FAST [12] taking into account all physical effects influencing the FEL amplifier operation (diffraction effects, energy spread, emittance, slip-

Table 3
Parameters of the sideband-seeded X-ray SASE FEL (Phase 1)

Radiator undulator	
Type	planar
number of periods	150
period, cm	2.73
peak field, T	0.51
external beta-function, m	1.7
Grating monochromator	
resolution, %	0.5-1
efficiency, %	10
wavelength range, nm	10-40
Output radiation after monochromator	
wavelength, nm	10-40
min. pulse duration, fs (FWHM)	30
number of photos per pulse	10^{11}
spectrum width, % (FWHM)	0.5

page effect, etc). It has been found that all complications do not violate the principle of the sideband generation and result in a correction of the output characteristics only, as usually takes place when going over from 1-D to 3-D FEL model. The results of optimized configuration of 20 nm sideband-seeded option of SASE FEL at the TESLA Test Facility are summarized in Table 3. Initial conditions for the seeded sideband have been fixed with general case, i.e. the slice of the electron bunch is modulated in energy and in density at the entrance to the X-ray undulator (see Figs.. 13 and 14). First we consider the case of uniform undulator, i.e. there is no sideband radiator undulator tuned to the sideband frequency. Figure 19 shows the evolution of the energy in the radiation pulse versus the undulator length. Saturation occurs at the undulator length of about 13 m. Temporal structure of the radiation pulse at saturation is shown in Fig. 20. Right plot in this Figure presents time structure of the radiation pulse after spectral filtering at the sideband frequency. Comparison with Fig. 17 shows that one-dimensional approximation provides visible overestimation of the radiation power at the sideband. However, absolute value is still high enough and is about one megawatt within fs pulse.

Next problem is that of optimization of the seeded sideband FEL consisting of the main undulator and the radiator tuned to the sideband frequency. Optimal length of the main undulator is given by the condition of maximum spectral purity of the sideband. In the case under study optimal length of the

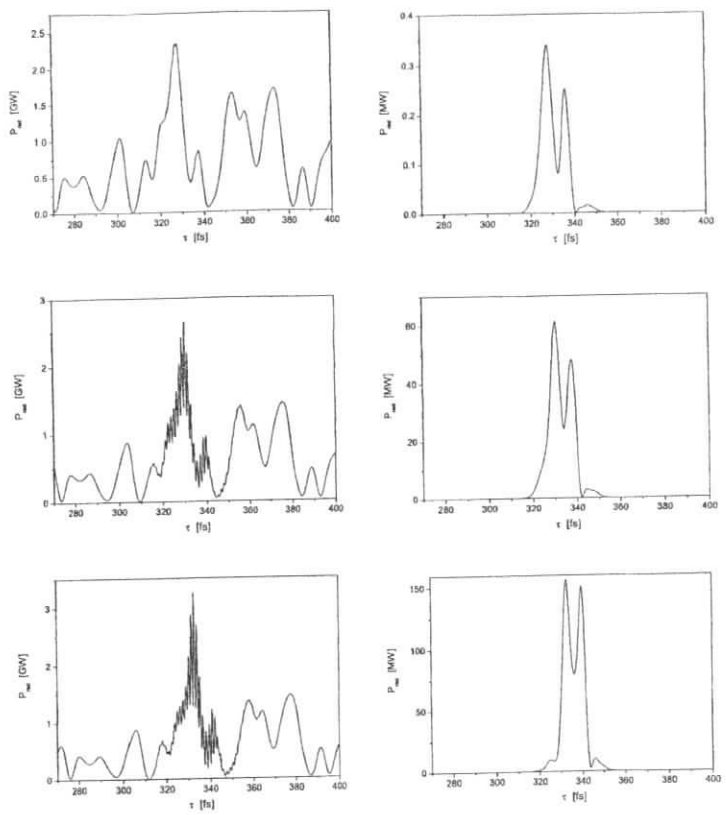

Fig. 21. Evolution of the radiation pulse in the radiator undulator. In the left plots we present total pulse, and in the right plots – spectrally filtered at the sideband. The length of the radiator undulator is equal to 0, 1 and 2 m for upper, middle and lower plots, respectively. Calculations have been performed with three-dimensional, time-dependent simulation code FAST.

main undulator should is equal to 10 m. Figures 21 and 22 show the evolution of the fs radiation pulse in the sideband radiator undulator. Figure 23 shows evolution of the spectral distribution of the output radiation power in the sideband radiator. Analysis of the spikes of the complete radiation pulse (plots in the left column of Figs. 21 and 22) shows that the radiation, produced in the main undulator, does not interact with the electron beam. Only that slice of the electron bunch, seeded by the sideband, produces the radiation. Cut structure of the spikes of the central part of the beam is due to the

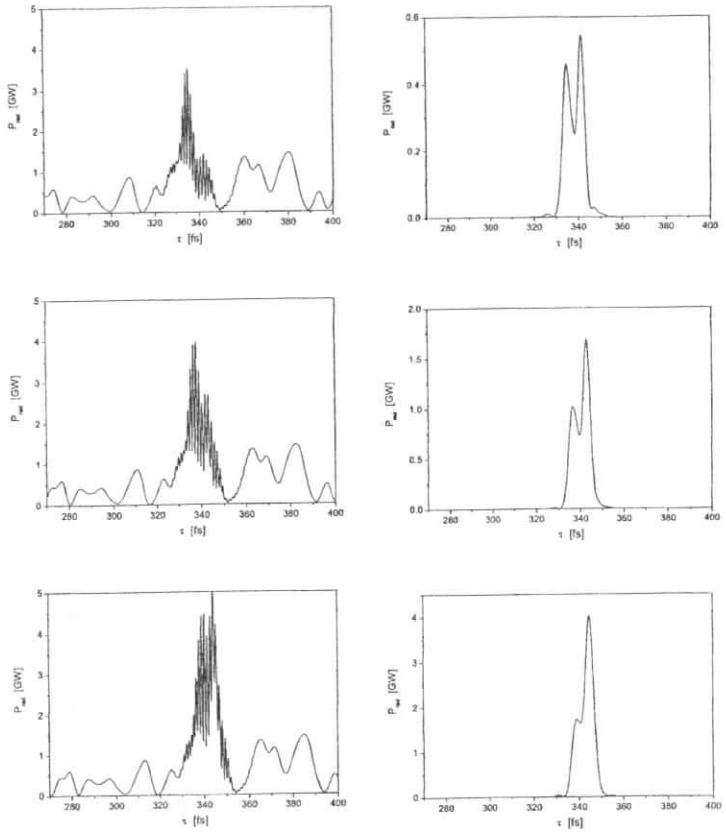

Fig. 22. Evolution of the radiation pulse in the radiator undulator. In the left plots we present total pulse, and in the right plots – spectrally filtered at the sideband. The length of the radiator undulator is equal to 3, 4 and 5 m for upper, middle and lower plots, respectively. Calculations have been performed with three-dimensional, time-dependent simulation code FAST.

interference of the radiation form the main undulator with frequency ω and from the sideband radiator with frequency $\omega - \omega_{opt}$. After 5 m long sideband radiator the radiation power in fs pulse rapidly reaches the level of a few GW, and the energy in the fs pulse reaches the value of about 30 μJ (see Fig. 24). Further increase of the radiator undulator does not lead to significant increase of the power, while the contrast of fs pulse starts to reduce drastically because of sideband growth in the nonlinear regime. Total undulator length of the

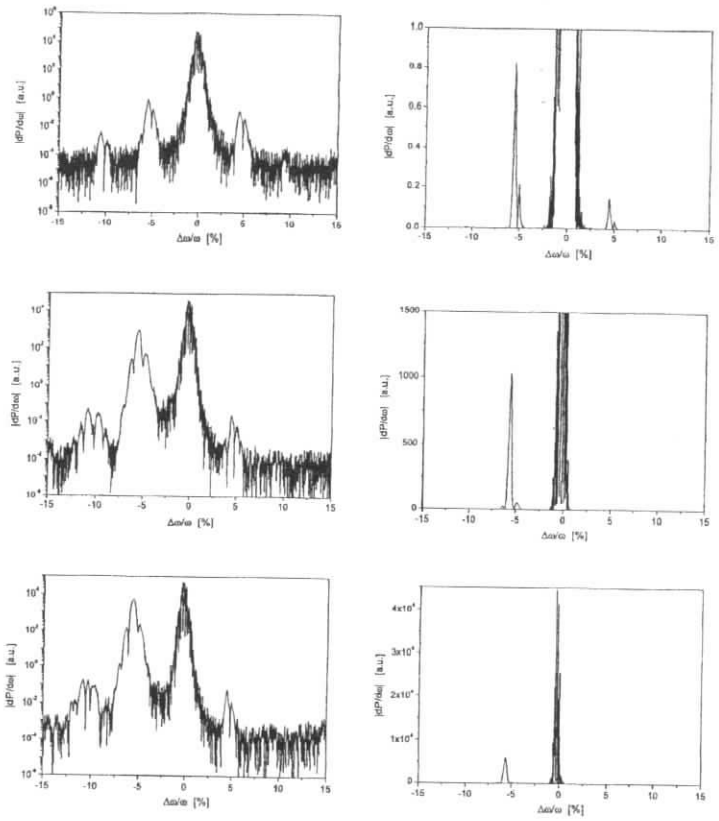

Fig. 23. Evolution of the spectral distribution of the output radiation power in the radiator undulator. In the left plots we present spectrum in logarithmic scale, and in the right plots – in the linear scale. The length of the radiator undulator is equal to 0, 3 and 5 m for upper, middle and lower plots, respectively. Calculations have been performed with three-dimensional, time-dependent simulation code FAST.

sideband seeded SASE FEL is about 15 meters.

In conclusion to this section we should note that calculations of the radiation power (see Figs. 20 – 24) have been performed for the case of an ideal monochromator. In the wavelength range of 10–40 nm the monochromator efficiency is about 10 per cent only, so the radiation power available for user experiments is roughly by one order of magnitude less than that shown in Figs. 20 – 24.

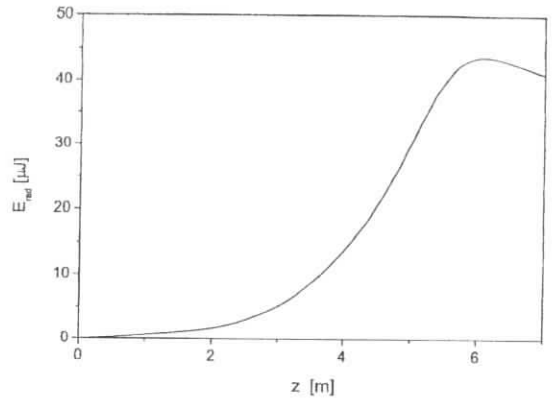

Fig. 24. Energy in a fs pulse versus length of the radiator undulator. Calculations have been performed with three-dimensional, time-dependent simulation code FAST.

Acknowledgments

We thank J.R. Schneider and D. Trines for their interest in this work and support.

References

[1] R. W. Schoenlein et al., Science 287(2000)2237

[2] W. Brefeld et al., DESY Print TESLA-FEL 2001-01, Hamburg 2001

[3] C. Pellegrini, Nucl. Instrum. and Methods A 445(2000)124

[4] W. Brefeld et al., DESY Print TESLA-FEL 2001-02, Hamburg 2001

[5] J. Rossbach, Nucl. Instrum. and Methods A 375(1996)269

[6] J. Feldhaus et al., Optics Communications 140(1997)341

[7] "Seeding Option for the VUV Free Electron Laser at DESY": Proposal. Available at DESY by request only

[8] "Development of a pump-probe facility with sub-picosecond time resolution combining a high-power optical laser and a soft X-ray free electron laser": Joint DESY (Germany), Forschungszentrum Juelich (Germany), Max-Born-Institute Berlin (Germany), Dublin City University (Ireland), MAX-Lab/Lund

Laser Center (Sweden) and CNRS/LURE, Orsay (France) Proposal. Available at DESY by request only

[9] Jean-Claude Diels and Wolfgang Rudolph "Ultrashort Laser Pulse Phenomena" Academic Press, New York, 1996

[10] D. Attwood, "Soft X-ray and Extreme Ultraviolet Radiation" Cambridge University Press, 1999

[11] E. L. Saldin, E. A. Schneidmiller and M. V. Yurkov, "The physics of Free Electron Lasers" Springer-Verlag, Berlin, 1999

[12] E. L. Saldin, E. A. Schneidmiller and M. V. Yurkov, Nucl. Instrum. and Methods A 429(1999)233